

Automatic Target Recognition and Tracking Filter

Jeffery R. Layne, Ph.D.
AFRL/SNAT, Bldg. 620
2241 Avionics Circle
WPAFB, Ohio 45433-7318
laynejr@sensors.wpafb.af.mil

ABSTRACT

The goal of the research is to develop a multiple model extended Kalman filter to perform simultaneous target identification and tracking using high range resolution (HRR) radar measurements. The idea is to use a multiple model estimator (MME) with multiple Kalman filters (one for each target type) to process HRR measurements. The resulting algorithm will provide estimates of the target kinematics (e.g. position, velocity, and possibly acceleration) and predict model probabilities, which correspond to the target probability. Hence, the approach proposed here is named the automatic target recognition (ATR) and tracking filter.

1. 0 INTRODUCTION

In most modern avionics systems, target tracking and target identification are typically dealt with as independent systems. However, we believe that there exists significant cross correlation in the information between these systems. Consequently, tightly coupling them should provide significant improvement in the overall performance. This paper shows one possible approach for correctly handling the cross correlations that might exist between target tracking and identification algorithms.

To motivate the problem further, consider the following example where kinematic information might help identification of a target. Assume we know that a given target is moving 400 Knots, then we can conclude that it is not likely a tank as they don't move that fast. Further, as shown in [1], kinematic information can be used to reduce the search space of a conventional template based ATR algorithm. Here kinematic information can be mapped to an approximate aspect angle. As a result, we only need to search the template space around the indicated aspect angle.

Likewise, target identification can aid tracking algorithms. For example, target type information can be used to significantly improve the process of associating radar observations with target tracks in a tracking algorithm. If we know the types of two closely spaced (or crossing) targets, it becomes easier to associate the observation to the correct target track. Further, as will be shown in this paper, it is possible to extract a pseudo-cross sectional length measurement from an HRR profile that is usually used for automatic target recognition. Assuming a specific target type, this "length" measurement can be mapped to a set of possible aspect angles. It will be shown that this observed aspect angle is correlated to the kinematics of the target thus providing an additional measurement for the tracking filter.

1.1 APPROACH

In approaching this problem, it is important to note that the problem consists of estimating continuous space kinematics and discrete space target type. Hence the approach should be an optimal one that is capable of dealing with both types of information. One such unified approach is the multiple model estimator presented in [2,3]. In this paper, we will investigate using the multiple model estimator to solve this problem.

Here we develop a multiple model extended Kalman filter to perform simultaneous target identification and tracking using high range resolution (HRR) radar. The idea is to use multiple Kalman filters (one for each target type) to process HRR measurements to estimate target kinematics (e.g. position, velocity, and possibly acceleration) and model probabilities, which correspond to the target probabilities.

REPORT DOCUMENTATION PAGE			Form Approved OMB No. 0704-0188		
Public reporting burden for this collection of information is estimated to average 1 hour per response, including the time for reviewing instructions, searching existing data sources, gathering and maintaining the data needed, and completing and reviewing this collection of information. Send comments regarding this burden estimate or any other aspect of this collection of information, including suggestions for reducing this burden to Department of Defense, Washington Headquarters Services, Directorate for Information Operations and Reports (0704-0188), 1215 Jefferson Davis Highway, Suite 1204, Arlington, VA 22202-4302. Respondents should be aware that notwithstanding any other provision of law, no person shall be subject to any penalty for failing to comply with a collection of information if it does not display a currently valid OMB control number. PLEASE DO NOT RETURN YOUR FORM TO THE ABOVE ADDRESS.					
1. REPORT DATE (DD-MM-YYYY) 01-01-1998		2. REPORT TYPE Conference Proceedings		3. DATES COVERED (FROM - TO) xx-xx-1998 to xx-xx-1998	
4. TITLE AND SUBTITLE Automatic Target Recognition and Tracking Filter Unclassified			5a. CONTRACT NUMBER		
			5b. GRANT NUMBER		
			5c. PROGRAM ELEMENT NUMBER		
6. AUTHOR(S) Layne, Jeffery R. ;			5d. PROJECT NUMBER		
			5e. TASK NUMBER		
			5f. WORK UNIT NUMBER		
7. PERFORMING ORGANIZATION NAME AND ADDRESS AFRL/SNAT Bldg. 620 2241 Avionics Circle Wright-Patterson AFB, OH45433-7318			8. PERFORMING ORGANIZATION REPORT NUMBER		
9. SPONSORING/MONITORING AGENCY NAME AND ADDRESS Director, CECOM RDEC Night Vision and Electronic Sensors Directorate, Security Team 10221 Burbeck Road Ft. Belvoir, VA22060-5806			10. SPONSOR/MONITOR'S ACRONYM(S)		
			11. SPONSOR/MONITOR'S REPORT NUMBER(S)		
12. DISTRIBUTION/AVAILABILITY STATEMENT APUBLIC RELEASE					
13. SUPPLEMENTARY NOTES See Also ADM201041, 1998 IRIS Proceedings on CD-ROM.					
14. ABSTRACT The goal of the research is to develop a multiple model extended Kalman filter to perform simultaneous target identification and tracking using high range resolution (HRR) radar measurements. The idea is to use a multiple model estimator (MME) with multiple Kalman filters (one for each target type) to process HRR measurements. The resulting algorithm will provide estimates of the target kinematics (e.g. position, velocity, and possibly acceleration) and predict model probabilities, which correspond to the target probability. Hence, the approach proposed here is named the automatic target recognition (ATR) and tracking filter.					
15. SUBJECT TERMS					
16. SECURITY CLASSIFICATION OF:		17. LIMITATION OF ABSTRACT Public Release	18. NUMBER OF PAGES 15	19. NAME OF RESPONSIBLE PERSON Fenster, Lynn lfenster@dtic.mil	
a. REPORT Unclassified	b. ABSTRACT Unclassified	c. THIS PAGE Unclassified		19b. TELEPHONE NUMBER International Area Code Area Code Telephone Number 703767-9007 DSN 427-9007	
				Standard Form 298 (Rev. 8-98) Prescribed by ANSI Std Z39.18	

The ATR and tracking filter algorithm takes advantage of *a priori* information such as the knowledge that one has that the velocity vector for ground targets is out the nose of the vehicle. In the case of air targets the acceleration vector is out the top of the aircraft when one assumes coordinated turns. Each filter takes as its input the target's cross sectional length measurement (provided by the HRR) and for a given target type assumed by each filter maps it to some set of target aspect angles. The filter processes the aspect angle that is most consistent with the kinematic estimate provided by that filter. If over time the aspect angles are very consistent with a target kinematics then the residuals for that filter will become very small. Likewise, if the aspect angles are not consistent with the kinematic information then the residuals become large. Therefore, the probability for each model (or target) is computed based on the size of the residuals for the given filter model.

The ATR and tracking filter discriminates between target types by constraining the kinematic estimate within the range of possibilities that the target is capable of performing. For example, we know that a tank cannot perform a 4g maneuver and move at 400 Knots. Consequently, we constrain the filter model for the tank such that accelerations cannot exceed the acceleration and velocity constraints for the given vehicle. If the HRR observations require acceleration and velocity estimates that exceed these constraints, then again the residuals for the given model become large thus reducing the target likelihood.

1.2 RELATED LITURATURE

The multiple model estimator approach presented in this paper is closely related to a method presented by Libby in [4] and Libby and Maybeck in [5]. Here Libby and Maybeck suggest using a multiple model estimator for processing synthetic aperture radar (SAR) measurements. In this research, the aspect angle is extracted using SAR measurements of length and width of the target.

Another related approach is presented by Jacobs and O'Sullivan in [6] and in the work of Kastella in [7]. The approach is based on the use of a nonlinear filter. Here the probability density for the target kinematic state and target type is computed by propagating the target's state via the Fokker-Plank equations. Given incoming radar measurement, the probability density is updated using Bayes rule.

Although the nonlinear filter approach correctly deals with system non-linearities and non-Gaussian probabilities, it does suffer a few problems for this application. First, the target kinematics are well characterized by linear systems and Gaussian distributions, which are easily handled by a Kalman filter. Further, the Fokker-Plank equations are inherently applicable only to continuous space systems. Thus the approach does not correctly handle the fact that this is a combined continuous and discrete space problem. Finally, the solution to the Fokker-Plank equation is very difficult to obtain since the resulting densities are usually complex in nature making them difficult to parameterize. To capture these complex density functions most solutions to the Fokker-Plank equations require the state space to be discretized. This results in very large computational complexity and approximate solutions (i.e. the solution is less than optimal).

1.3 PAPER OVERVIEW

This paper is organized in the following fashion. Section 2 presents an overview of HRR radar measurements and presents a discussion of the errors that corrupt these measurements. Section 3 presents the architecture of the multiple model estimator (MME). Section 4 presents both the propagation and update equations that must be implemented in the design of the extended Kalman filters used in the MME. Section 5 presents some simulation results for both the ATR and tracking filter and provides a comparison to a similar conventional tracking algorithm. Finally, Section 6 presents some concluding remarks and discusses future research directions.

2. 0 HIGH RANGE RESOLUTION RADAR MEASUREMENTS

High range resolution radar combined with monopulse radar processing is capable of measuring range, range rate, azimuth angle, and elevation angles along the line-of-sight vector from the aircraft to the target. These observations are the ones traditionally used in a tracking filter. In addition to these, we will extract one other observation for use in the ATR and tracking filter that we call the pseudo cross sectional length of the target. Next, we discuss some of these measurements in detail.

The vector geometry defining the azimuth angle (A) and elevation (E) angle is shown in Figure 1. Here, the azimuth angle is defined to be the angle between a vector pointing along the y -axis and the line-of-sight vector. The elevation angle is defined to be the angle between a vector pointing along the z -axis and the line-of-sight vector. The coordinate frame shown in Figure 1 will be discussed in more detail later in this section.

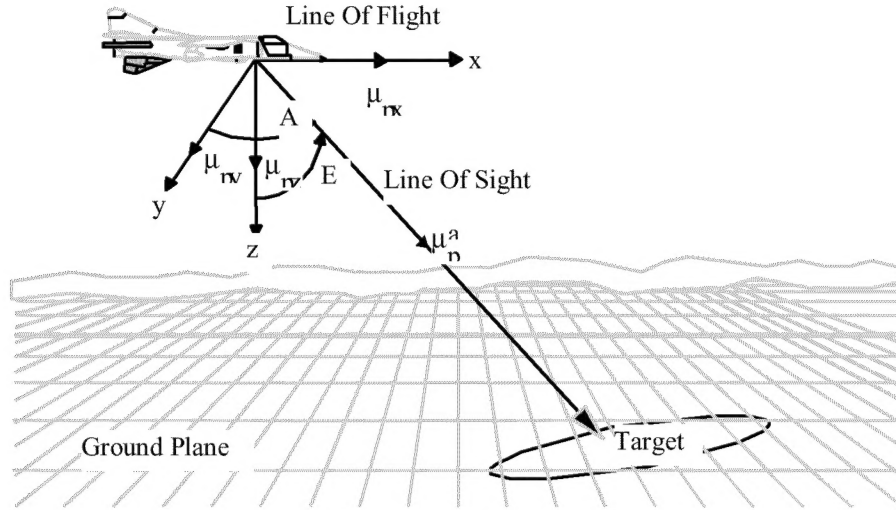


Figure 1. Radar geometry.

The “pseudo” cross sectional length, denoted L_c , is extracted from the HRR profile. As shown in Figure 2, the cross sectional length is obtained by observing the number of range bins in sequence whose value exceeds some threshold. This measurement can be obtained somewhat accurately as a result of Doppler filtering the background clutter and coherent integration of multiple radar pulses in HRR measurements. However, we refer to it as the “pseudo” cross sectional length as it can sometimes be severely corrupted by radar effects such as multipath.

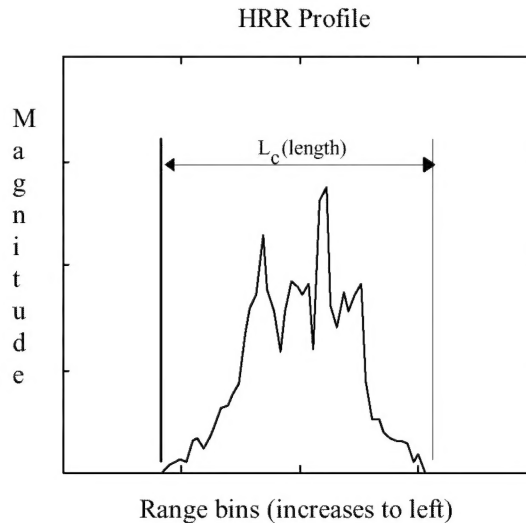


Figure 2 – A typical HRR profile.

For a given target type and depression angle, the cross sectional length can be mapped to a set of possible aspect angles. As shown in Figure 3, the aspect angle for ground based targets is the angle between the vector pointing out the nose of the target and the line of sight vector projected onto the ground plane. Figure 4 illustrates a case for the M35 truck where a pseudo cross sectional length of 30 maps to a set of four possible aspect angles.

The observed aspect angle that is closest to the one predicted by the Kalman filter for the M35 truck is the one that is processed by the ATR and tracking filter. This point should become clear in the next section of the paper.

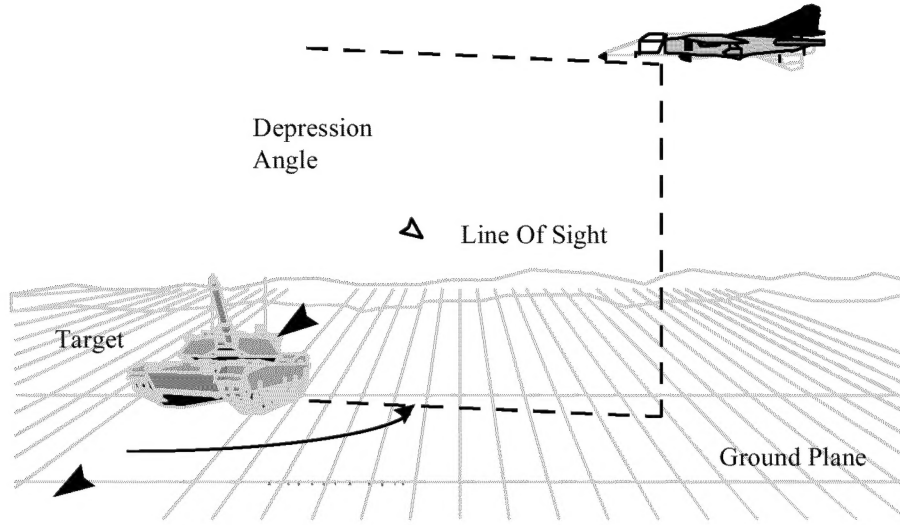


Figure 3 - Aspect angle geometry.

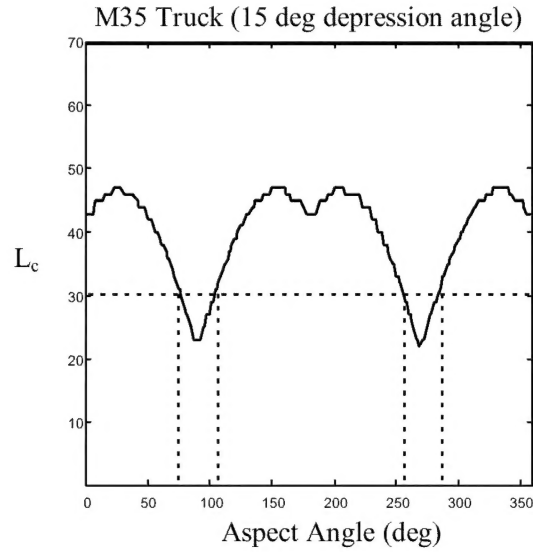


Figure 4 – A plot of the target length profile as a function of aspect angle for a M35 truck.

2.1 MEASUREMENT TRUTH MODELS

As previously mentioned, a high range resolution radar coupled with monopulse radar processing is capable of measuring range, range rate, azimuth angle, elevation angle, and pseudo cross sectional length to a given target. These measurements are not perfect and are typically modeled as the sum of true value and the measurement errors. Hence, the range measurement, denoted z_T , and range rate measurement, denoted \dot{z}_T , are modeled by the following equations:

$$z_T = r + \delta r_{CL} + r\delta C + v_{rQ} + v_{rT} + v_{rOT}, \quad (1)$$

$$z_T = \dot{r} + \delta \dot{r}_D + \dot{r} \delta C + \dot{r} \delta F + v_{r_Q} + v_{r_T} + v_{r_{OT}}, \quad (2)$$

respectively, where r is the true range, \dot{r} is the true range rate, and the other error terms are described in Table 1. For an electronically scanned array antenna (ESA), which we now assume, the measured azimuth angle, denoted z_A , and elevation angle, denoted z_E , are modeled by the following equations:

$$z_A = A + \delta A_{TEMP} + v_{A_{MA}} + v_{A_{FL}} + v_{A_{PU}} + v_{A_{CC}} + v_{A_{MS}} + v_{A_{TN}} + v_{A_Q} + v_{A_{RAD}} \quad (3)$$

$$z_E = E + \delta E_{TEMP} + v_{E_{MA}} + v_{E_{FL}} + v_{E_{PU}} + v_{E_{CC}} + v_{E_{MS}} + v_{E_{TN}} + v_{E_Q} + v_{E_{RAD}}, \quad (4)$$

where A and E are the true azimuth and elevation angles, respectively, and the other error terms are described in Table 1.

Since we had real measured HRR profiles to use in this study, it was not necessary to develop a stochastic model for the pseudo cross sectional length measurement. The data we used consisted of HRR profiles for aspect angles on the interval $[0, 360]$ degrees at approximately 1 to 2 degree increments for both 15 and 17-degree depression angles. Since we did not have HRR profiles for all depression angles, we assumed that the true depression angle remained at 17 degrees for the entire simulation and the measured depression angle was 15 degrees. What is suggested by this approximation is that the targeting aircraft is changing pitch in such a way that the depression angle is constant. Although this assumption is not very realistic; we believe it is an approximation that does not severely effect the final result.

3.0 ARCHITECTURE OF THE ATR AND TRACKING FILTER

In the ATR and tracking filter, it is assumed that the system dynamics obeys one of a finite number of fixed models (one for each target type). Figure 5 shows the architecture for the ATR and tracking filter. The overall output estimate, usually referred to as the combined estimate, is the weighted sum of the estimates from each model.

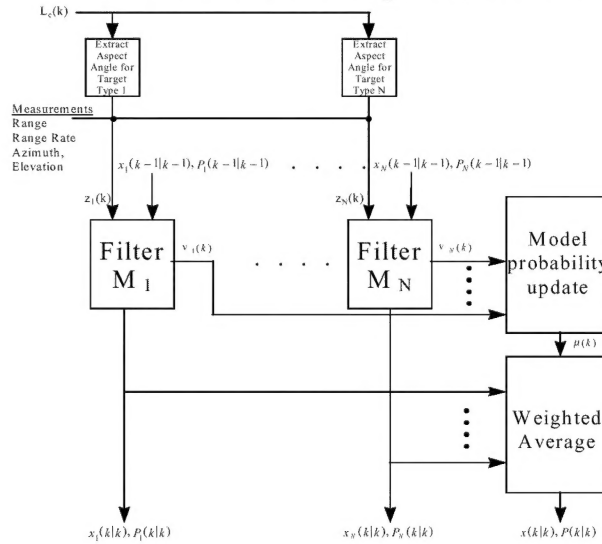


Figure 5. ATR and tracking filter architecture.

Table 1. Summary of Radar Error Budget

Symbol For Error	Description Of Error Source	RMS Value	Correlation Time
δr_{CL}	Range Clock Error	0.01 feet	bias

δC	Propagation Speed Error	10 PPM	bias
δr_D	Range Rate Doppler Error	0.001 ft/s	bias
δF	Frequency Error	20 PPM	bias
v_{rQ}	Range Quantization Error	$\Delta r / \sqrt{12}$	white
v_{rT}	Range Timing Error ¹	$T_d \dot{r}$	white
v_{rOT}	Range Miscellaneous Errors ²	$0.5 \Delta r$	white
\dot{v}_{rQ}	Range Rate Quantization Error	$\Delta r / \sqrt{12}$	white
\dot{v}_{rT}	Range Rate Timing Error	$T_d \dot{r}$	white
\dot{v}_{rOT}	Range Rate Miscellaneous Errors ³	$0.5 \Delta \dot{r}$	white
δA_{TEMP}	Azimuth Temperature Induced Errors and Antenna Misalignment.	1.08 <i>mrad</i>	bias
δE_{TEMP}	Elevation Temperature Induced Errors and Antenna Misalignment.	1.08 <i>mrad</i>	bias
v_{AMA}	Azimuth Mechanical Alignment Error	0.30 <i>mrad</i>	white
v_{EMA}	Elevation Mechanical Alignment Error	0.30 <i>mrad</i>	white
v_{AFL}	Azimuth Flexure Error	0.10 <i>mrad</i>	white
v_{EFL}	Elevation Flexure Error	0.10 <i>mrad</i>	white
v_{APU}	Azimuth Radome Phase Uniformity Error	0.35 <i>mrad</i>	white
v_{EPU}	Elevation Radome Phase Uniformity Error	0.35 <i>mrad</i>	white
v_{ACC}	Azimuth Rx Channel Cross Coupling Error	0.15 <i>mrad</i>	white
v_{ECC}	Elevation Rx Channel Cross Coupling Error	0.15 <i>mrad</i>	white
v_{AMS}	Azimuth Monopulse Slope Error	0.10 <i>mrad</i>	white
v_{EMS}	Elevation Monopulse Slope Error	0.10 <i>mrad</i>	white
v_{ATN}	Azimuth Thermal Noise	0.20 <i>mrad</i>	white
v_{ETN}	Elevation Thermal Noise	0.20 <i>mrad</i>	white
v_{AQ}	Azimuth Quantization Error	0.20 <i>mrad</i>	white
v_{EQ}	Elevation Quantization Error	0.20 <i>mrad</i>	white
v_{ARAD}	Azimuth Radome Error	0.40 <i>mrad</i>	white
v_{ERAD}	Elevation Radome Error	0.40 <i>mrad</i>	white

3.1 FILTER MODEL

In this research, we assume that the fixed models are in the form of a stochastic difference equation describing the system behavior. For example, the model $\{M_j; j=1, \dots, N\}$ is given by

¹ T_d is the processing time delay (1 ms).

² Δr is the range resolution of the radar (100 feet).

³ The range rate resolution $\Delta \dot{r}$ is a function of the angular rate of the aircraft about the target, denoted ω , and the azimuth resolution of the radar, denoted Δaz , such that $\Delta \dot{r} = \omega \Delta az$. For the results presented in this paper the azimuth resolution was (100 feet)

$$\hat{x}_j(k+1) = \Phi \hat{x}_j(k) + \Gamma a_j(k), \quad (5)$$

where $\hat{x}_j(k) \in \mathbb{R}^n$ is the filter's state vector, $a_j(k) \in \mathbb{R}^m$ is the fixed input,. In the truth model $a_j(k)$ is assumed to be corrupted by a white noise vector $w(k) \in \mathbb{R}^m$ such that $w(k) \sim N(0, Q)$. The matrices $\Phi \in \mathbb{R}^{n \times n}$ and $\Gamma \in \mathbb{R}^{n \times m}$ are the state transition matrix and the measurement matrix, respectively.

The measurements or observations are modeled as non-linear functions of the state. For example assume that the j^{th} filter uses a non-linear estimate of the measurements Then it can be expressed by the following equation

$$\hat{z}_j(k) = h_j(\hat{x}_j, k). \quad (6)$$

When designing an extended Kalman filter, it is necessary to linearize the measurement equations to obtain the filter's observation matrix, denoted H_j . The filter's observation matrix is obtained by computing a first order Taylor series approximation of the filter's estimate of the measurement equations. For example, consider the general non-linear estimate of the measurement given by Equation 5. The first order Taylor series approximation of this equation is given by the following

$$\hat{z}_j(k) = z_{j0} + \frac{\partial h_j(\hat{x}_j, k)}{\partial \hat{x}_j} \delta \hat{x}_j, \quad (7)$$

where z_{j0} is the true value of the measured quantities (e.g. true range). Equation 7 can be written more compactly

$$\hat{z}_j(k) = z_{j0} + H_j \delta \hat{x}_j \quad (8)$$

where

$$H_j = \frac{\partial h_j(\hat{x}_j, k)}{\partial \hat{x}_j} \quad (9)$$

3.2 KALMAN FILTERING

The updates for the j^{th} , $\{j=1, N\}$, filter model are computed via the Kalman filter equations using the mixed estimate and covariance

$$\hat{x}_j(k|k-1) = \Phi \hat{x}_j(k-1|k-1) + \Gamma a_j(k) \quad (10)$$

$$P_j(k|k-1) = \Phi P_j(k-1|k-1) \Phi^T + \Gamma Q_j \Gamma^T \quad (11)$$

$$S_j(k) = H_j P_j(k|k-1) H_j^T + R_j \quad (12)$$

$$v_j(k) = z_j(k) - \hat{z}_j(k|k-1) \quad (13)$$

$$K_j(k) = P_j(k|k-1) H_j^T S_j^{-1} \quad (14)$$

$$P_j(k|k) = P_j(k|k-1) - K_j(k) H_j P_j(k|k-1) \quad (15)$$

$$\hat{x}_j(k|k) = \hat{x}_j(k|k-1) + K_j(k) v_j(k) \quad (16)$$

where $x_j(k|k) \in \mathbb{R}^n$ is the state estimate for this model, $P_j(k|k) \in \mathbb{R}^{n \times n}$ is the covariance of the state estimate error, $v_j(k) \in \mathbb{R}^m$ is the innovation process, $S_j(k) \in \mathbb{R}^{m \times m}$ is the covariance of the innovation process, and $K_j(k) \in \mathbb{R}^{n \times m}$ is the Kalman filter gain.

3.3 MODEL PROBABILITY

The likelihood function of model M_j : $\{j = 1, \dots, N\}$ at time k , under the linear Gaussian assumption is

$$\Lambda_j(k) = p[z_j(k)|Z^{k-1}, M_j] = p[v_j(k)] = N[v_j(k); 0, S_j(k)], \quad (17)$$

where $N(x; m, P)$ is a Gaussian density function of on x with mean m and covariance P . The posterior probability of model j being correct is obtained recursively

$$\mu_j(k) = \frac{\Lambda_j(k) \mu_j(k-1)}{c} \quad j = 1, \dots, N, \quad (18)$$

where the normalizing constant c is given by

$$c = \sum_{i=1}^N \Lambda_i(k) \mu_i(k-1). \quad (19)$$

This recursive algorithm is started at $\mu_j(0)$ specified *a priori*.

3.4 ESTIMATE AND COVARIANCE COMBINATION

The estimated probability density function of the system state is the weighted average of the N model estimates, i.e. the overall mean is given by

$$\hat{x}(k|k) = \sum_{j=1}^N \mu_j(k) \hat{x}_j(k|k), \quad (20)$$

and overall covariance given by

$$P(k|k) = \sum_{j=1}^N \mu_j(k) P_j(k|k). \quad (21)$$

4.0 ATR AND TRACKING FILTER DESIGN

In tracking systems it is possible to track targets in many possible coordinate systems. For this paper we chose to track targets in a Cartesian coordinate system attached to the aircraft's body. Tracking in *body* frame coordinates is useful when one is concerned only with the location of the target relative to the aircraft. However, if one desires to pass the target's location to another user (e.g. the case of a hunter-shooter scenario), it becomes necessary to express the target location in some commonly known coordinates such as an earth-centered earth-fixed coordinate system. In this case it would be necessary to model and simulate errors related to our navigation system. As depicted in Figure 1, the body frame has its origins at the aircraft's center such that x points out the nose of the aircraft, y points out the right side of the aircraft, and z points out the bottom of the aircraft. In this section, we present the propagation and measurement equations for the extended Kalman filter design under the

assumption that we are tracking in body frame coordinates. This includes a presentation of the derived linear observation matrix H .

4.1 KALMAN FILTER PROPAGATION EQUATIONS

In this research we assume that the fixed models are of the form of nearly constant velocity models with a bias corresponding to acceleration. In other words, the stochastic difference equation describing the system behavior for model $\{M_j; j=1, \dots, N\}$ is given by Equation (5) where

$$\hat{\mathbf{x}}_j(k) = [\hat{p}_x(k) \hat{p}_y(k) \hat{p}_z(k) \hat{v}_x(k) \hat{v}_y(k) \hat{v}_z(k)]^T \quad (22)$$

is the filter's state vector consisting of the target's position and velocity component and

$$\mathbf{a}_j(k) = [a_{jx}(k) \ a_{jy}(k) \ a_{jz}(k)]^T \quad (23)$$

is the acceleration vector. The state transition matrix $\Phi \in \mathbb{R}^{6 \times 6}$ and measurement matrix $\Gamma \in \mathbb{R}^{6 \times 3}$ are given by

$$\Phi = \begin{bmatrix} \mathbf{I}_{3 \times 3} & T\mathbf{I}_{3 \times 3} \\ \mathbf{0} & \mathbf{I}_{3 \times 3} \end{bmatrix}, \text{ and} \quad \Gamma = \begin{bmatrix} \frac{T^2}{2}\mathbf{I}_{3 \times 3} \\ T \mathbf{I}_{3 \times 3} \end{bmatrix},$$

respectively, where T is the discrete time sample period and $\mathbf{I}_{n \times n} \in \mathbb{R}^{n \times n}$ is an identity matrix.

4.2 FILTER'S ESTIMATE OF HIGH RANGE RESOLUTION RADAR MEASUREMENTS

The filter's estimate of the range, denoted \hat{r} , from the aircraft to the target is the magnitude of the line of sight vector estimate, denoted $\hat{\mathbf{p}}$. Thus range is found by computing the 2-norm of the line of sight vector.

$$\hat{r} = \sqrt{(\hat{\mathbf{p}})^T \hat{\mathbf{p}}} \quad (24)$$

The range rate is found by computing the time derivative of the range. Upon performing this operation we obtain

$$\dot{\hat{r}} = -(\hat{\mathbf{u}}_p)^T \hat{\mathbf{v}}, \quad (25)$$

where $\hat{\mathbf{u}}_p$ is the unit look vector between the aircraft and the target and $\hat{\mathbf{v}}$ is the relative velocity vector. The unit look vector is expressed as:

$$\hat{\mathbf{u}}_p = \frac{\hat{\mathbf{p}}}{\|\hat{\mathbf{p}}\|} = \frac{\hat{\mathbf{p}}}{\sqrt{(\hat{\mathbf{p}})^T \hat{\mathbf{p}}}}. \quad (26)$$

To compute the filter's estimate of the azimuth and elevation angles, consider the unit vectors $\hat{\mathbf{u}}_{py}$ and $\hat{\mathbf{u}}_{pz}$ which point in the body frame y and z directions, respectively. These vectors are expressed as

$$\hat{\mathbf{u}}_{py} = [0 \ 1 \ 0]^T \quad (27)$$

$$\hat{\mathbf{u}}_{pz} = [0 \ 0 \ 1]^T. \quad (28)$$

The relationship between the vectors of interest and the filter's estimate of the azimuth and elevation angles are given by

$$\cos(\hat{A}) = (\hat{\mathbf{u}}_p)^T \hat{\mathbf{u}}_{py} \quad (29)$$

$$\cos(\hat{E}) = (\hat{\mathbf{u}}_p)^T \hat{\mathbf{u}}_{pz} \quad (30)$$

Solving for \hat{A} and \hat{E} yields

$$\hat{A} = \cos^{-1} [(\hat{\mathbf{u}}_p)^T \hat{\mathbf{u}}_{py}] \quad (31)$$

$$\hat{E} = \cos^{-1} [(\hat{\mathbf{u}}_p)^T \hat{\mathbf{u}}_{pz}] \quad (32)$$

where both \hat{A} and \hat{E} lie in the interval $[0, \pi]$ radians.

To compute the filter's estimate of the aspect angles, denoted $\hat{\theta}$, we must first convert the position vector $\hat{\mathbf{p}}$ to heading frame coordinates. The heading frame is a local level frame whose origin is located at the aircraft's center. The x^h axis points in the direction of the local level component of the velocity vector. The z^h axis points down toward the reference ellipsoid and the y^h axis is tangent to the reference ellipsoid. The body frame defines the attitude of the aircraft's body relative to the heading frame via roll, pitch, and yaw angles α_x , α_y , and α_z that are estimated by the navigation system. The coordinate transformation from body frame to heading frame coordinates is given below. In order to write the results compactly, we abbreviated cos by C and sin by S .

$$C_b^h = \begin{bmatrix} C\alpha_z C\alpha_y & C\alpha_z S\alpha_y S\alpha_x - S\alpha_z C\alpha_x & C\alpha_z S\alpha_y C\alpha_x + S\alpha_z S\alpha_x \\ S\alpha_z C\alpha_y & S\alpha_z S\alpha_y S\alpha_x + C\alpha_z C\alpha_x & S\alpha_z S\alpha_y C\alpha_x - C\alpha_z S\alpha_x \\ -S\alpha_y & C\alpha_y S\alpha_x & C\alpha_y C\alpha_x \end{bmatrix} \quad (33)$$

To avoid modeling and simulating a full blown navigation system, we assumed that this coordinate transformation was known perfectly in the simulation results presented later in this paper.

The line of sight vector, $\hat{\mathbf{p}}$, in body frame coordinates can be transformed to heading frame vector, denoted $\hat{\mathbf{p}}^h$, by the following equation

$$\hat{\mathbf{p}}^h = C_b^h \hat{\mathbf{p}} \quad (34)$$

At this time, we will make a simplifying assumption that the ground plane is level at the target. This assumption could be avoided if we had digital terrain and elevation data (DTED) available to determine the gradient vector. Now consider the vector $\hat{\mathbf{p}}_{xy}$, which is the line of sight vector projected onto the ground plane. This vector is expressed as

$$\hat{\mathbf{p}}_{xy} = [\hat{p}_x^h \ \hat{p}_y^h \ 0]^T \quad (35)$$

where \hat{p}_x^h and \hat{p}_y^h are the x and y components, respectively of the line of sight vector, $\hat{\mathbf{p}}^h$, in heading frame coordinates. Now normalize this vector to obtain a unit vector, $\hat{\mathbf{u}}_{pxy}$ pointing in the same direction.

$$\hat{\mathbf{u}}_{pxy} = \frac{\hat{\mathbf{p}}_{xy}}{\sqrt{(\hat{\mathbf{p}}_{xy})^T \hat{\mathbf{p}}_{xy}}}. \quad (36)$$

The velocity vector in heading frame coordinated is given by

$$\hat{\mathbf{v}}^h = \mathbf{C}_b^h \hat{\mathbf{v}} \quad (37)$$

Thus the unit velocity vector in heading frame coordinates is given by

$$\hat{\mathbf{u}}_v = \frac{\hat{\mathbf{v}}^h}{\|\hat{\mathbf{v}}^h\|} \quad (38)$$

The relationship between the unit vector, $\hat{\mathbf{u}}_{pxy}$, the relative unit velocity vector, $\hat{\mathbf{u}}_v$, and the filter's estimate of the aspect angle, $\hat{\theta}$, is given by

$$\cos(\hat{\theta}) = -(\hat{\mathbf{u}}_{pxy})^T \hat{\mathbf{u}}_v. \quad (39)$$

Solving for $\hat{\theta}$ yields

$$\hat{\theta} = \cos^{-1} [-(\hat{\mathbf{u}}_{pxy})^T \hat{\mathbf{u}}_v] \quad (40)$$

where $\hat{\theta}$ lies on the interval $[0, 2\pi]$ radians.

Since we do not include error states in the Kalman filter models, the filter's estimate of the measurements are simply the filter's estimate of the range, range rate, azimuth angle, elevation angle, and aspect angle, i.e.,

$$\hat{z}_r = \hat{r}, \quad (41)$$

$$\hat{z}_{\dot{r}} = \dot{\hat{r}}, \quad (42)$$

$$\hat{z}_A = \hat{A}, \quad (43)$$

$$\hat{z}_E = \hat{E}, \quad (44)$$

$$\hat{z}_\theta = \hat{\theta}. \quad (45)$$

4.3 THE FILTER'S OBSERVATION MATRIX

As previously mentioned, when designing an extended Kalman filter, it is necessary to linearize the measurement equations to obtain the filter's observation matrix. This observation matrix is obtained by computing a first order Taylor series approximation of the filter's estimate of the measurement equations. For the high-resolution radar measurements presented in this paper, the filter's observation matrix is similar to that presented in [8,9,10,11,12] with the addition of the aspect angle measurement. The components that make up H_j , the j^{th} filter's observation matrix are summarized in

Table 2. The terms $\hat{\delta \mathbf{p}}$ and $\hat{\delta \mathbf{v}}$ are the position and velocity errors, respectively, for the j^{th} filter and all the other components are computed based on the j^{th} filter's estimate.

Table 2 - Filter observation matrix (H_i).

H_i	$\delta \hat{\mathbf{p}}$	$\delta \hat{\mathbf{v}}$
\hat{z}_r	$(\hat{\mathbf{u}}_p)^T$	$\mathbf{0}$
$\hat{z}_{\dot{r}}$	$(\hat{\mathbf{v}})^T \hat{\mathbf{L}}$	$(\hat{\mathbf{u}}_p)^T$
\hat{z}_A	$\hat{\nabla}_A^T$	$\mathbf{0}$
\hat{z}_E	$\hat{\nabla}_E^T$	$\mathbf{0}$
\hat{z}_θ	$\hat{\nabla}_p^T C_b^h$	$\hat{\nabla}_v^T C_b^h$

$$\hat{\mathbf{L}} = -\frac{1}{\hat{r}}[\mathbf{I} - \hat{\mathbf{u}}_p(\hat{\mathbf{u}}_p)^T] \quad (46)$$

$$\hat{\nabla}_A^T = \frac{-(\hat{\mathbf{u}}_{py})^T}{\hat{r} \sin(\hat{A})} [\mathbf{I} - \hat{\mathbf{u}}_p(\hat{\mathbf{u}}_p)^T] \quad (47)$$

$$\hat{\nabla}_E^T = \frac{-(\hat{\mathbf{u}}_{pz})^T}{\hat{r} \sin(\hat{E})} [\mathbf{I} - \hat{\mathbf{u}}_p(\hat{\mathbf{u}}_p)^T] \quad (48)$$

$$\hat{\nabla}_p^T = \frac{-(\hat{\mathbf{u}}_v)^T}{\|\hat{\mathbf{p}}_{xy}\| \sin(\hat{\theta})} [\mathbf{I} - \hat{\mathbf{u}}_{pxy}(\hat{\mathbf{u}}_{pxy})^T] ; \hat{\nabla}_{\theta pz} = 0 \quad (49)$$

$$\hat{\nabla}_v^T = \frac{-(\hat{\mathbf{u}}_{pxy})^T}{\|\hat{\mathbf{v}}\| \sin(\hat{\theta})} [\mathbf{I} - \hat{\mathbf{u}}_v(\hat{\mathbf{u}}_v)^T] \quad (50)$$

5.0 SIMULATION RESULTS

In this section, we compare the performance of our ATR and tracking filter to a classical tracking filter which processes only range, range rate, azimuth angle, and elevation angle. For the simulation results presented in this section, the target was a M35 truck with the target track shown in Figure 6. In our ATR and tracking filter design, we used 11 models representing the following target types: a BMP-2 tank, a BTR-70 transport, a HMMVW, a M1 tank, a M109 gun, a M110 gun, a M113 transport, a M2 tank, a M35 truck, a M548 transport, and a T72 tank.

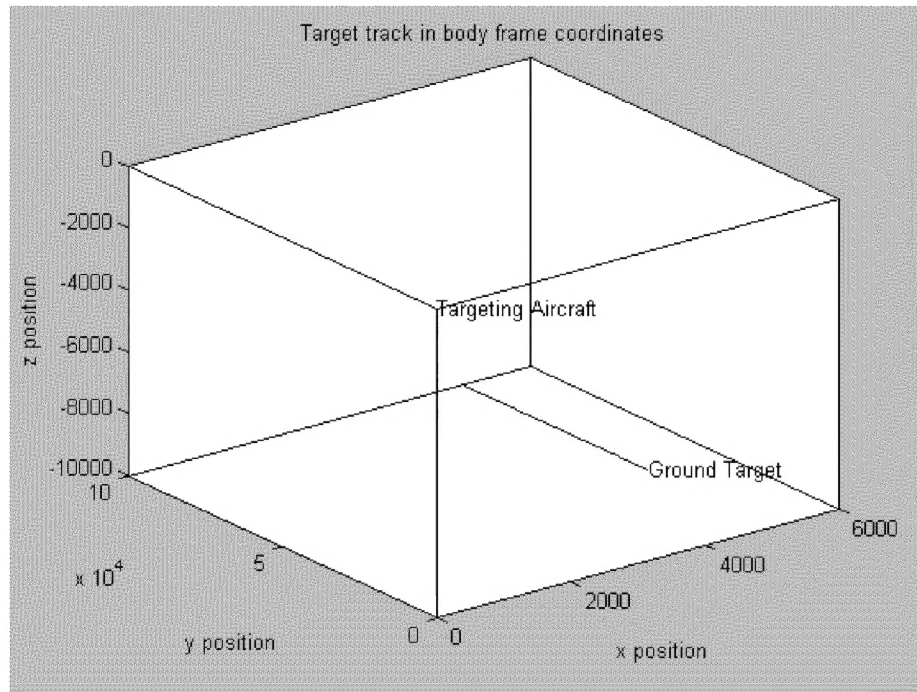


Figure 6 – True target track in body frame coordinates.

For both algorithms, we computed the 10 Monte Carlo run average RMS error for the x , y , and z position and velocity. The results are shown in Table 3. Notice in Table 3 that the average RMS errors for our ATR and tracking filter is considerably smaller than those obtained for the classical tracking filter. This is especially true in the x and z directions which we believe is due to the geometry in this scenario.

Table 3 - 10 Monte Carlo Run ensemble average RMS error

	Classical Tracking Filter	HRR-ATR and Tracking Filter
x position	153.63	113.09
y position	47.99	47.91
z position	56.40	46.80
x velocity	45.95	14.72
y velocity	22.94	22.88
z velocity	23.60	15.41

Figure 7 shows the 10-run average target probabilities for this simulation. Since the M35 truck and the M2 Tank are approximately the same size, the algorithm initially had some difficulty in deciding the true target type. However, as time progressed in the simulation, the ATR and tracking algorithm managed to accrue enough evidence to correctly identify the target as a M35 truck. The plot in Figure 7 represents typical performance for the ATR and tracking filter algorithm. We found that for other targets the algorithm performed significantly better or somewhat worse.

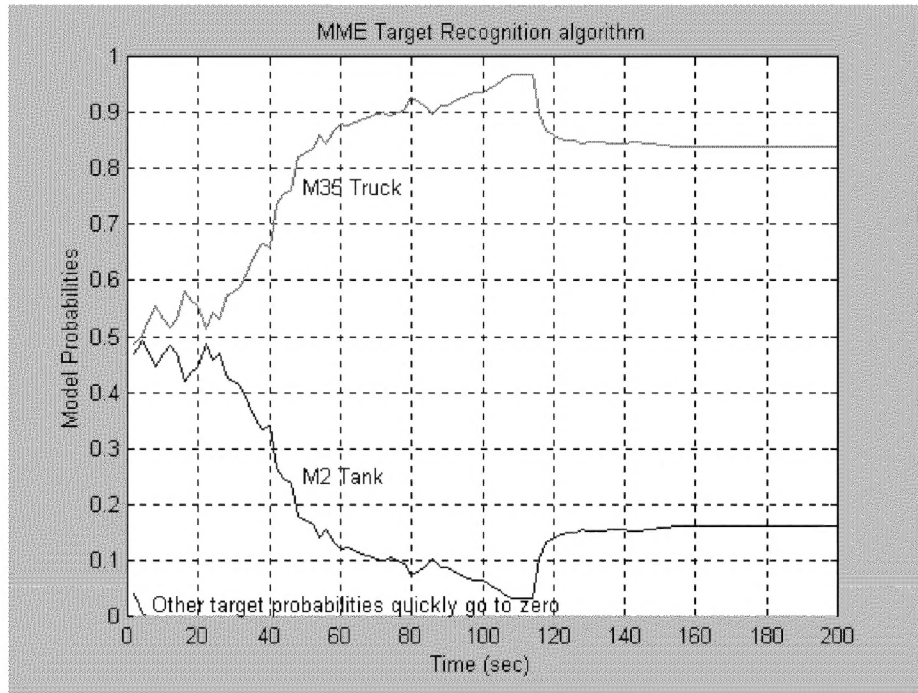


Figure 7 – Plot of 10 run ensemble average of target model probabilities.

6.0 CLOSING REMARKS

The purpose of this paper was to motivate a combined ATR and tracking system and to present the framework and illustrate the performance of a combined ATR and tracking filter. The results show that, by processing a pseudo cross-sectional length measurement in the ATR and tracking filter, we obtain improved tracking performance while gaining information on target type.

Future research will focus on two topics. First, we plan to “fuse” the results of a conventional Gaussian discriminate HRR-ATR algorithm with that of the ATR and tracking filter algorithm into a unified and tightly coupled approach. An optimal method for doing this has already been formulated. Doing this should provide significant improvement to both the model probability and the track accuracies. Second, we plan to formulate a track association scheme that takes advantage of the target type information provided by the ATR and tracking filter.

REFERENCES

1. R. Williams, J. Westerkamp, D. Wardell, S. Worrell, and M. Ressler, "Robustness issues for 1D ATR," Proceedings of the Sixth ATR Working Group Systems and Technology Symposium, Redstone Arsenal, Alabama, October 1997.
2. J. Gustafson and P. Maybeck, "Control of a large flexible space structure with moving-bank multiple model adaptive algorithms," *Proceedings of the 31st Conference on Decision and Control*, Tucson, Arizona, pp. 1273-1278, December, 1992.
3. P. Maybeck and K. Hentz, "Investigation of moving-bank multiple model adaptive algorithms," *AIAA Journal of Guidance, Control, and Dynamics*, Vol. 10, No. 1, pp. 90-96, Jan./Feb. 1987.
4. E. Libby, "Application of sequence comparison methods to multisensor data fusion and target recognition," Ph.D. Dissertation, Air Force Institute of Technology, June, 1993.
5. E. Libby and P. Maybeck, "Application of sequence comparison methods to multisensor data fusion and target recognition," *Aerospace and Electronics Systems*, pp 52-65, January, 1996.
6. S. Jacobs and J. O'Sullivan, "High-resolution radar models for joint tracking and recognition," *Proceedings of the 1997 IEEE National Radar Conference*, pp 99-104, May, 1997.
7. K. Kastella and A. Zatezalo, "A nonlinear filter for real-time joint tracking and recognition," *Aerospace and Electronics Systems*, (Submitted), 1997.
8. S. Musick, "Radar measurements and measurement matrices," Tech. Rep. AFAL-TM-76-48, Wright Laboratory (AFMC), Wright Patterson AFB, Ohio, May 1976.
9. J. Layne and E. Blasch, "Integrated synthetic aperture radar and navigation systems for targeting applications," Tech. Report, Wright Laboratory (AFMC), Wright Patterson AFB, Ohio, September 1997.
10. J. Layne and U. Piyasena, "Adaptive interacting multiple model tracking of maneuvering targets," *Proceedings of the 16th Digital Avionics Systems Conference*, Irvine, California, October, 1997.
11. J. Layne, "Monopulse radar tracking using an adaptive interacting multiple model method with extended Kalman filters," *Aerospace and Electronics Systems*, (Submitted), 1997.
12. J. Layne, "Monopulse radar tracking using an adaptive interacting multiple model method with extended Kalman filters," *SPIE Signal and Data Processing of Small Targets*, Orlando, Florida, April, 1998.